Superfluid onset and prewetting of ^{4}He on rubidium

J. A. Phillips, D. Ross, P. Taborek, and J. E. Rutledge
Department of Physics and Astronomy, University of California, Irvine, California 92697-4575
(Received 13 March 1998)

Quartz-crystal microbalance isotherms of ^{4}He on rubidium are presented. The isotherms are used to locate the prewetting transition and the onset of superfluidity in the adsorbed helium films. The phase diagram of He on Rb is distinctly different from helium on either conventional strong substrates or on cesium. In particular, the superfluid transition is hysteretic and does not conform to the Kosterlitz-Thouless paradigm. [S0163-1829(98)04930-3]

I. INTRODUCTION

Films of ^{4}He adsorbed on solid surfaces have been studied for many years and a standard picture of their properties on most surfaces has been established.[1] The interaction between a ^{4}He film and nearly all surfaces is so strongly attractive that the first one or two atomic layers of the film are solidified or otherwise localized. Subsequent layers remain fluid and become superfluid at low temperature. The experimentally observed signatures of superfluid onset are remarkably independent of the properties of the substrate; the two-dimensional superfluid transition has the same characteristics whether it occurs on solid hydrogen, Mylar, or gold. Similarly, the standard Kosterlitz-Thouless (KT) model[2,3] used to describe the superfluid transition in films is strictly two dimensional and is independent of the boundary conditions at the substrate. The KT picture has been extremely successful in quantitatively explaining the shear response,[4] thermal conductivity,[5] and third sound modes[6] of ^{4}He films near superfluid onset on a variety of substrates.

Recently, alkali-metal surfaces have proven to be radically different adsorption substrates for ^{4}He and other simple gases. Adsorption potentials for ^{4}He on the alkali metals are ''weak,'' which means that the potential well formed by the competition between long-range van der Waals attraction and short-range Pauli repulsion has a depth comparable with the binding energy of a ^{4}He atom in the bulk fluid. The phases of helium on alkali-metal substrates have been theoretically analyzed by Cheng, Cole, Saam, and Treiner.[7] Their analysis has been confirmed by experiments on the weakest substrate, cesium. Cs is nonwet at low temperatures and wet above a wetting temperature near 2 K. Between 2 K and about 2.5 K it displays a prewetting transition,[8] a first-order phase transition on the vapor side of the bulk liquid-vapor coexistence curve marked by two-phase equilibrium between thin and thick films. The effects of first-order prewetting on the KT transition have also been investigated.[9] In the case of thin cesium substrates, the KT line terminates on the prewetting phase boundary at a critical end point. For temperatures above the critical end point, prewetting and the KT transition are distinctly different transitions. Below the critical end point, the KT transition does not exist and prewetting is a direct transition between a thin normal phase and a thick superfluid phase. Since the thin phase is always normal on Cs, superfluid onset can only be studied above the wetting temperature.

There have been several previous investigations of ^{4}He adsorption on Rb. Rubidium is a slightly stronger substrate than Cs, and is theoretically expected to have a lower wetting temperature.[7,10] A lower wetting temperature provides an experimental opportunity to study superfluid onset over a wider temperature range. Superfluid onset on weak substrates is particularly interesting because even the first adsorbed ^{4}He layer is expected to remain fluid so the inert layer of solidified helium that forms on strong substrates can be avoided.[7]

There have also been experimental investigations of ^{4}He adsorption on Rb.[11–14] The most extensive of these studies have utilized heat-flow measurements to map the superfluid onset. This type of experiment can detect transitions to a superfluid state, but, as shown in Ref. 9, superfluid onset and prewetting are not necessarily coincident phase transitions. In this paper, we report experimental observations of both the wetting and superfluid properties of ^{4}He films on Rb using the quartz microbalance technique. Characteristic features in the frequency shift and the dissipation allow us to construct a phase diagram showing the boundaries between thick and thin and superfluid and normal phases. Above 1.9 K, prewetting and superfluid onset are distinct phase transitions, while below this temperature, the transitions are strongly coupled. At temperatures below 1.9 K, superfluid onset on Rb is surprisingly different from the Cs case investigated in Ref. 9. Although the superfluid transition on Rb retains Kosterlitz-Thouless-type features, the transition is hysteretic and the size and temperature dependence of the features do not conform to the universal predictions of the KT theory. Another important practical difference between Rb and Cs is that our technique for producing alkali-metal substrates is less reproducible for Rb. Isotherms on Rb films evaporated and annealed in nominally the same way had features whose location was reasonably well defined, but whose height, width, and shape varied substantially from one substrate to another.

This paper is organized as follows. Section II contains a discussion of the experimental procedures, including the techniques used for preparing the Rb substrates and a description of a method for determining the chemical potential at low temperatures when the vapor pressure is too low to measure directly. In Sec. III, we present the data, which consist primarily of measurements of the frequency shift and the

dissipation of the quartz microbalance as a function of ^{4}He chemical potential at constant T. A number of these isotherms from 0.15 to 2.2 K are used to assemble a μ-T phase diagram that shows the relationship between the prewetting line and the KT transition line.[15] Measurements of the superfluid density and dissipation at onset show that in many cases, superfluid transitions on Rb do not follow the standard KT model. Evidence of two types of behavior in the thin-film phase above and below 0.3 K is also presented. In Sec. IV we discuss the wetting and superfluid onset behavior of ^{4}He on Rb and compare it to results obtained with Cs and conventional strong substrates such as Au. The possibility that the KT line meets the prewetting line in a multicritical point and the possible role of substrate disorder are also considered. Finally, Sec. V provides a summary of our findings.

II. EXPERIMENTAL METHODS

The response of high-Q mechanical oscillators to an adsorbed helium film has been an important probe of both prewetting and superfluid onset.[4,5,8,9,16–22] The experiments reported here utilize AT cut quartz oscillators as microbalances. The microbalances consist of a quartz substrate shaped like a thin convex lens about 1 cm in diameter and 0.1 cm thick. A gold electrode covers the center of each side and defines the mass-sensitive area. When a voltage is applied to the electrodes, opposite faces of the crystal move transversely to the thickness of the device at a third harmonic of 5.5 MHz. Since the quartz microbalances oscillate in a shear mode, in a first approximation only the viscously clamped normal fraction of the helium film, including any solid layers that may be present, will couple to the substrate. When the film undergoes the normal-to-superfluid transition, one sees a sharp step in the resonant frequency because of the decoupling of the zero-viscosity superfluid film from the substrate. Another signature of the superfluid transition in helium films is a peak in the dissipation $(1/Q)$. A quantitative understanding of these effects is based on a finite frequency modification of static KT theory.[3]

In an electrical circuit, a quartz microbalance is equivalent to a damped series LC resonant circuit with a resonant frequency f and real part of the impedance R. Adsorbed films shift the resonant frequency from the vacuum value by an amount proportional to the film mass Δf. Losses in the film shift the real part of the impedance by ΔR. If the crystals were planar and infinite in diameter, their motion would be strictly transverse with opposite faces moving parallel to themselves. In real devices the resonant modes necessarily contain a small admixture of motion perpendicular to the faces.[23] This means that even at low temperatures where the superfluid fraction is virtually 1, the devices retain some sensitivity to variations in the adsorbed mass. Depending on the oscillator, 10–20% of the superfluid couples to the microbalance. This provides a detection sensitivity of 0.025–0.05 Hz/layer of superfluid compared with a sensitivity of 0.25 Hz/layer of normal liquid ^{4}He.

Rubidium adsorption surfaces are prepared by evaporating vacuum-distilled rubidium metal over the gold electrodes of a microbalance. During evaporation and subsequent annealing, the substrate and experimental cell are maintained below 6 K to ensure ultrahigh vacuum conditions. The data reported here were obtained on three different Rb surfaces. Surfaces 1 and 3 had 75 layers of Rb evaporated on each side of the microbalance and were then annealed near 80 K for half an hour. Surface 2 was prepared in two stages, each of which consisted of evaporating 38 layers per side and annealing at 80 K for half an hour.

The cell is cooled by a dilution refrigerator and connected through a capillary to a source of high-purity helium gas. It is also connected to a pumping system through a much larger tube and a cold valve. This configuration allows us to add ^{4}He to the cell at any temperature and to remove it above 0.7 K. At lower temperatures the removal rate is prohibitively low.

Our raw data consist of adsorption isotherms measured at temperatures between 0.15 and 2.2 K. They are presented as plots of Δf and ΔR as functions of the pressure or the chemical potential offset from saturation $\Delta\mu$. Depending on the vapor pressure, the chemical potential is determined in one of three ways. Above 1.2 K the pressure is measured by a room-temperature capacitive manometer. Between 0.8 and 1.2 K the pressure is measured by an *in situ* capacitance gauge calibrated against the room-temperature manometer. In these cases $\Delta\mu$ was calculated from the pressure using the ideal gas approximation $\Delta\mu=\mu-\mu_0=T\ \ln(P/P_0)$. Here μ_0 and P_0 are the chemical potential and pressure at liquid-vapor coexistence, respectively. When an isotherm is performed below 0.8 K, the vapor pressure is too low to be measured by either one of the pressure gauges and another method must be used.

For the low-temperature isotherms we make use of a second microbalance in the experiment cell that has standard gold electrodes. On this strong substrate, it is plausible that the coverage (or equivalently Δf) is a function of only $\Delta\mu$, and not of T and P separately. This conjecture has been experimentally verified for ^{3}He and used for low-temperature chemical potential measurements in a previous study.[24] The application of the technique for ^{4}He is complicated by the fact that the superfluid fraction of the adsorbed film is temperature dependent and the sensitivities of the microbalance to superfluid and normal fluid are different. Because of this difference, Δf is not simply proportional to the coverage, and plots of Δf as a function of $\Delta\mu$ for various temperatures yield a family of distinct curves. It is possible, however, to collapse this family of curves onto a single universal curve by making a suitable correction for the sensitivity of the microbalance to the superfluid.

The sensitivity to the superfluid is obtained by measuring several isotherms at high enough temperatures that the previously mentioned pressure gauges can be used to determine the chemical potential. The isotherms can be normalized by considering the frequency shift Δf_n that would be measured if the film had the same thickness but was entirely normal fluid. Δf_n is related to the measured value Δf by

$$\Delta f_n=\frac{\Delta f}{\dfrac{\rho_N}{\rho}+k\,\dfrac{\rho_S}{\rho}}, \tag{1}$$

where ρ_N/ρ and ρ_S/ρ are the temperature-dependent normal and superfluid ratios, respectively, and k is the fraction of superfluid that couples to the oscillator. For a suitably chosen

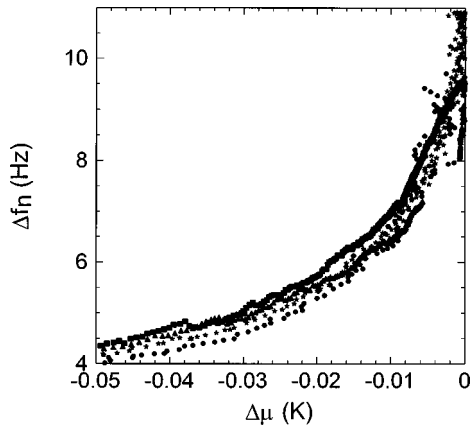

FIG. 1. The frequency shift Δf_n as a function of ^{4}He chemical potential $\Delta\mu$ on a gold surface for four temperatures. Δf_n is the frequency shift given by Eq. (1) that corrects for the uncoupled superfluid fraction. The 1.398-K isotherm is indicated by circles, the 1.218-K isotherm by stars, the 0.987-K isotherm by squares, and the 0.888-K isotherm by triangles. Note that all the data fall on a universal curve. We have used this relationship between Δf_n and $\Delta\mu$ as the basis for our chemical-potential measurements at low temperatures.

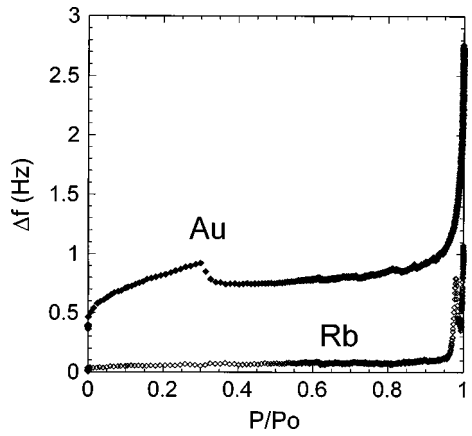

FIG. 2. Adsorption isotherm at 1.2 K of helium on gold and rubidium substrates as a function of vapor pressure. The gold oscillator's frequency shift indicates several layers of helium adsorbed at low pressure while the rubidium surface has less than a layer until near saturation. The film on the Au oscillator goes superfluid near 30% saturated vapor pressure while the film on the Rb surface does not become superfluid until $P/P_0=0.98$.

value of k (in our case $k=0.20$) isotherms taken over a wide range of temperature fall on a single curve when Δf_n is plotted as a function of $\Delta\mu$, as shown in Fig. 1. Similar values of the superfluid coupling factor were obtained in previous experiments on Mylar torsional oscillators,[4,5] while much larger values are observed on exfoliated graphite.[21] We assume that the functional dependence of Δf_n on $\Delta\mu$ does not change between 0.8 and 0.15 K. A line of best fit is drawn through the data to give the function needed to convert the gold oscillator's frequency shift to chemical potential at low temperatures (below 0.8 K). The uncertainty in $\Delta\mu$ in this method is approximately 5 mK.

III. DATA

In order to cover a large region of the μ-T plane, isotherms were performed from $T=0.15$ to 2.2 K in the pressure range from vacuum to liquid-vapor coexistence. Figure 2 shows a frequency shift isotherm at 1.2 K for both the Au and the Rb-coated oscillators. Note that the Au oscillator has a frequency shift corresponding to several adsorbed layers even at very low pressures, while the Rb oscillator shows less than one-half monolayer adsorption until quite near the saturated vapor pressure. In subsequent figures, we will usually omit the low-coverage, low-pressure regime and concentrate on the region near coexistence where the film thickness changes rapidly. In Fig. 3 we present a sample pair of isotherms performed at 1.50 K on surface 2. The figure shows the resonant frequency shift Δf and dissipation change ΔR as a function of $\Delta\mu$. The system started in vacuum and gas was slowly added to the experiment cell. This type of isotherm in which $\Delta\mu$ increases as a function of time is referred to as a ''forward'' isotherm and is indicated by the open diamonds in Fig. 3. At low chemical potential Fig. 3(a) indicates that at most only 0.2 ML are adsorbed. Near $\Delta\mu=-0.05$ K, Δf abruptly increases. This behavior is characteristic of a prewetting thick/thin transition. When the frequency shift reaches a value of 0.8 Hz (corresponding to a thickness of four layers), the film undergoes a superfluid transition. This transition is identified by two significant features: Δf drops as the superfluid fraction uncouples from the oscillator and ΔR has the predicted dynamic KT peak at the same $\Delta\mu$ [Fig. 3(b)]. As more helium is added to the cell, Δf continues to increase because the film thickness is rapidly

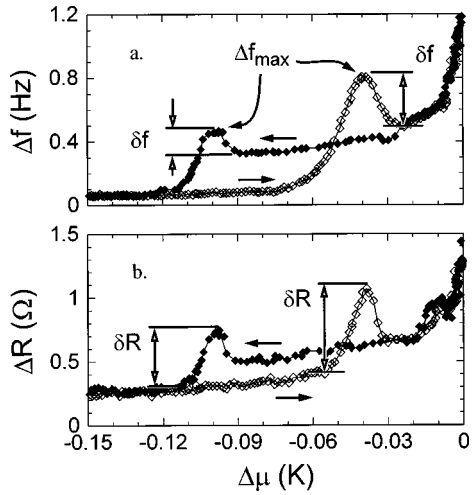

FIG. 3. Adsorption isotherms at 1.5 K of helium on rubidium surface 2 as a function of chemical potential offset from liquid-vapor coexistence $\Delta\mu$. Isotherms are hysteretic and depend on whether the chemical potential is increasing or decreasing. Open diamonds are a forward isotherm in which helium is added to the experiment cell. Solid diamonds are a reverse isotherm obtained by removing helium from the cell starting from liquid-vapor coexistence. (a) Frequency-shift isotherm. $\Delta f=0$ corresponds to vacuum. The rapid increase of Δf indicates a prewetting thin/thick transition. The peak in Δf near the transition is marked by $\Delta f_{\max}$. The frequency change due to viscous decoupling at the superfluid transition is indicated by δf. (b) Impedance shift ΔR of microbalance. The peaks in the impedance δR are the conventional indicators of a KT superfluid transition.

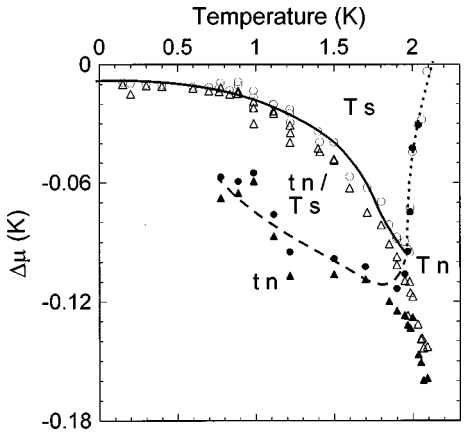

FIG. 4. Phase diagram for ^{4}He films on all three Rb substrates. Open circles are the normal-to-superfluid transitions in forward isotherms. Filled circles are superfluid transitions of reverse isotherms. Open and filled triangles mark the corresponding branches of the prewetting transition. Curves marking the phase boundaries are guides to the eye. The dotted line is the conventional KT transition that passes through the lambda point and the prewetting critical region. The solid curve marks the combined prewetting and superfluid onsets obtained from the forward isotherms. The dashed line marks the stability limit of the thick/thin and superfluid transitions obtained from the reverse isotherms. Regions of the phase diagram are indicated by the lettering scheme: *t*, thin; *T*, thick; *s*, superfluid; and *n*, normal.

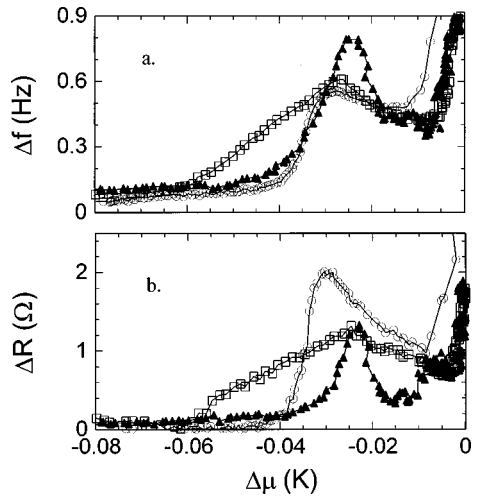

FIG. 5. Isotherms at 1.22 K on each of the three Rb surfaces studied in this paper. Surface 1 is indicated by circles, surface 2 by triangles, and surface 3 by squares. (a) Frequency shift of microbalances as a function of chemical potential. (b) Impedance shift of microbalance as a function of chemical potential. Note that the transition from thin-normal to thick-superfluid occurs at $\Delta\mu = -0.03 \pm 0.005$ K on each surface even though the values of δf and δR differ on each.

increasing and the oscillator has some nontransverse motion that couples to the superfluid film. Since the film ends up in a thick state at saturation, it is said to wet the rubidium.

We have systematically looked for hysteresis in the thin-normal to thick-superfluid transition by measuring ''reverse'' isotherms in which small amounts of helium gas are sequentially removed from the experiment cell. In Fig. 3, the reverse isotherm, denoted by solid diamonds, starts at coexistence in the thick-superfluid state and is coincident with the forward isotherm down to $\Delta\mu = -0.03$ K, where the two sets of data diverge. On the reverse isotherm, the film remains superfluid until $\Delta\mu = -0.10$ K, where the film first becomes normal (Δf and ΔR increase) and then goes through the prewetting transition to the thin state.

The data shown in Fig. 3 are typical of our data between 0.75 and 1.95 K. Throughout this range the forward and reverse $\Delta\mu$ values at prewetting and superfluid onset are strongly hysteretic. In addition, the superfluid onset thicknesses, the onset superfluid jumps, and the dissipation peak heights and areas are larger on the forward branch at each temperature. At 1.95 K the hysteresis abruptly decreases and the forward and reverse isotherms become nearly identical. Below 1.95 K the difference between the prewetting and superfluid onset $\Delta\mu$ values is small and roughly temperature independent. Above 1.95 K the $\Delta\mu$ difference rapidly grows, and prewetting and superfluid onset become clearly distinguishable transitions.

Isotherms from three rubidium substrates in the temperature range 0.15–2.2 K were used to construct a $\Delta\mu$-T phase diagram shown in Fig. 4. An open triangle marks the value of $\Delta\mu$ at the steepest point on the prewetting step and an open circle marks the position of the dissipation peak on the forward isotherm at each temperature. Corresponding solid symbols mark these features on the reverse isotherms. Some of the scatter in the points in Fig. 4 is due to variations among the three Rb surfaces; typical behavior of forward isotherms at $T = 1.22$ K for each of the three surfaces is shown in Fig. 5. Note that the peak occurs at approximately the same value of $\Delta\mu$ for each surface, but the size and shape of the peak varies from surface to surface.

The solid line in Fig. 4 connects the thin-to-thick transitions of the forward isotherms and will be referred to as the prewetting line. Notice that it does not intersect the liquid-vapor saturation line $\Delta\mu = 0$, implying that helium wets our rubidium surfaces at all temperatures. This conclusion does not depend on subtleties of our method of measuring $\Delta\mu$ at low temperature. After prewetting and superfluid onset, more gas must be added to the cell to reach saturation even at the lowest temperatures. This can clearly be seen in Fig. 6, which shows a plot of Δf as a function of the amount of gas admitted to the cell N for both the rubidium-coated oscillator and the bare gold oscillator at $T = 0.3$ K. The plateau in Δf vs N for the gold oscillator indicates a region of bulk liquid-vapor coexistence in which the adsorbed film has reached its asymptotic gravitationally limited thickness. The prewetting peak on the Rb oscillator occurs at substantially lower N than the coexistence value.

It is interesting to inquire whether the Kosterlitz-Thouless picture, which successfully describes superfluid onset on both conventional substrates and Cs, can also account for the combined superfluid/prewetting transition we observe on Rb. We find that although the basic features of a superfluid jump and enhanced dissipation clearly exist, the universal KT predictions do not apply to superfluid onset on Rb. Although the Kosterlitz-Thouless theory makes no explicit prediction about the absolute thickness of the film at superfluid onset, the jump in the superfluid fraction σ_s depends only on T and universal constants:[2]

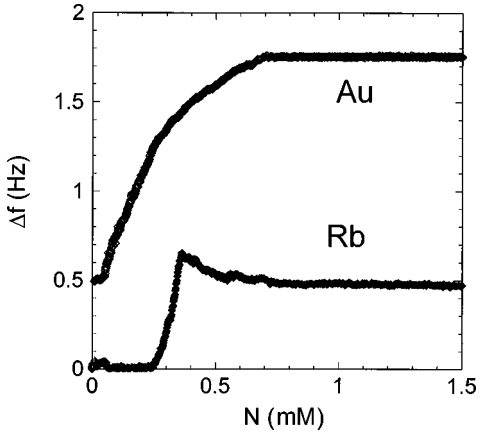

FIG. 6. Isotherms at 0.300 K for rubidium surface 2 (bottom curve) and gold (top curve). The frequency shifts of the microbalances are given as functions of the amount of helium added to the experiment cell in millimoles. The plateau in the Au curve that begins at 0.7 mM indicates that the experiment reached saturation after the Rb underwent the prewetting transition at 0.35 mM.

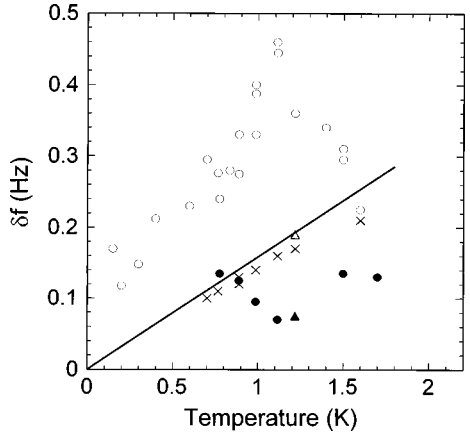

FIG. 7. Frequency jump due to superfluid transition in ^{4}He films as a function of temperature. Open circles are forward isotherms on surface 2, solid circles are reverse isotherms on the same surface. Open and solid triangles are forward and reverse isotherms on surface 3, and ×'s are isotherms on Au. The universal KT prediction is given by the straight line.

$$\sigma_S(T_C)=\frac{8\pi m k_B T_C}{h^2}, \tag{2}$$

where m is the mass of a helium atom, k_B is Boltzmann's constant, T_C is the transition temperature, and σ_S is the coverage in atoms/m^2. In terms of our experimental observables, this implies that the frequency shift at onset δf is numerically given by

$$\delta f=\left(\frac{-4f_n^2}{nR_q}\right)m\sigma_S(T_C)=(0.1584\ \text{Hz/K})T_C, \tag{3}$$

where f_n is the resonant frequency of the nth harmonic and R_q is the transverse acoustic impedance of quartz ($R_q \cong 8.862\times10^6$ kg/m^2 sec). This prediction is manifestly independent of the substrate. Furthermore, since the KT transition is a higher-order transition, it cannot be superheated or supercooled, so no hysteresis in the onset temperature is expected.

In our isotherms, the abrupt step in Δf on the thick-film side of the prewetting transition, denoted by δf in Fig. 3, can be attributed to a KT-like jump in the superfluid density. δf does not, however, obey the KT prediction of Eq. (2). For example, the data at 1.50 K (Fig. 3) show a superfluid jump of 0.35 Hz (1.4 layers) on the forward isotherm, while the reverse isotherm shows a jump of 0.18 Hz (0.7 layers). The fact that these two values are different is a violation of the KT prediction that the size of the jump is a unique function of T. Furthermore, neither of them is equal to the predicted value of 0.25 Hz (1.0 layer). A number of isotherms like Fig. 3 have been used to construct a plot of the magnitude of the superfluid jump at onset δf as a function of T for both forward and reverse branches on Rb for surfaces 2 and 3, as shown in Fig. 7. The universal KT prediction [straight line from Eq. (2)] and the δf vs T results from the gold oscillator, determined by the same method we used on the Rb oscillator, are shown for comparison. The agreement between the gold data and the KT prediction is typical of all previously studied surfaces,[9,16,18,25] and provides a check of our experimental procedure.

The temperature dependence of the dissipation peak associated with superfluid onset on Rb is also anomalous. The forward and reverse δR measurements on Rb for surfaces 1 and 2 and the δR values on Au are shown in Fig. 8. The dynamic KT prediction for the dissipation, although not universal, is proportional to T;[3] the expected straight-line behavior is also shown in Fig. 8. The reverse Rb dissipation peaks and the peaks on Au are similar and conform with the KT picture. However, the forward isotherm δR values grow rapidly with decreasing temperature and in fact appear to be diverging as T goes toward 0 K. Although the absolute value of the loss is different for the two surfaces, the trend of increasing loss with decreasing temperature is seen on both.

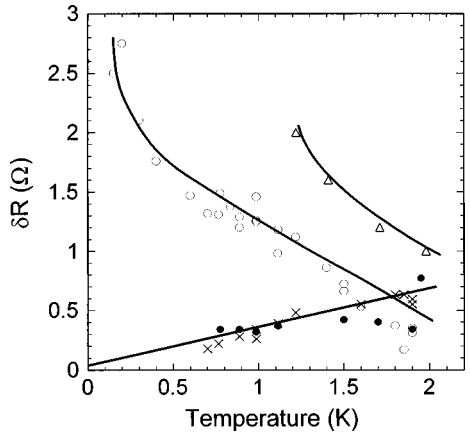

FIG. 8. Size of impedance peaks at superfluid transition in helium films as a function of temperature. ×'s are the peak size occurring on Au substrates. Solid circles are taken from reverse isotherms on Rb substrate 2. Open circles are from forward isotherms on surface 2 and open triangles on surface 1. The straight line is the predicted temperature behavior of the dynamic KT theory. The curves connecting the forward Rb data are guides to the eye indicating a divergent behavior at low temperature.

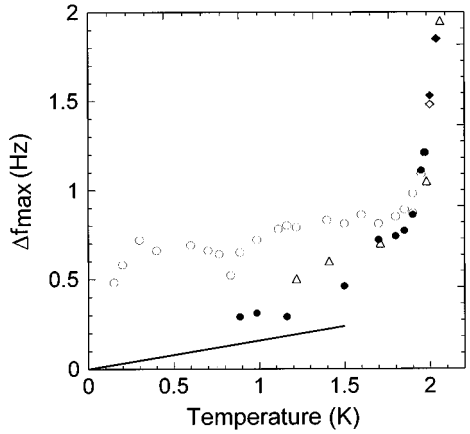

FIG. 9. Maximum frequency shift $\Delta f_{\max}$ just before superfluid onset as a function of temperature. The open circles indicate the onset thickness for the forward isotherms on surface 2 and solid circles are the reverse isotherms on the same surface. The open triangles are for the forward isotherms on surface 1. The forward and reverse data do not have the same onset thickness, and furthermore, neither curve extrapolates to $\Delta f_{\max}=0$ at $T=0$ K. The straight line indicates the predicted KT value if no solid or inert layers are present in the He given by $\Delta f_{\max}=\delta f$ from Eq. (3).

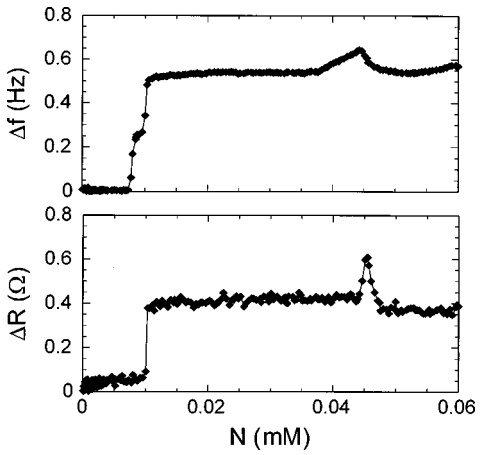

FIG. 10. Adsorption isotherm of He on a bare Au microbalance at 0.701 K. (Top) The frequency shift of the oscillator is shown as a function of the amount of gas injected into the experiment cell. Two solid layers of He form on the microbalance that is indicated by the two steplike features at $N=0.01$ mM. This layering is only observed on Au and not on Rb surfaces. At $N=0.045$ mM the portion of the helium film that is on top of the solid layers goes superfluid. This is indicated by the usual KT characteristic frequency drop due to the uncoupling of the superfluid fraction. (Bottom) The superfluid transition is also evident in the dissipation curve of the microbalance. There is a sharp peak in ΔR at the same $N=0.045$ mM as predicted by the dynamic version of KT theory.

On a conventional substrate, the minimum helium coverage required for superfluidity is considerably higher than the KT critical coverage defined in Eq. (2). This phenomenon is attributed to the existence of a solidlike ''dead layer'' that is immobilized by the substrate potential. This layer is typically about 2 ML thick, but on weak substrates such as solid hydrogen, the critical coverage for superfluidity at $T=0$ is approximately $\frac{1}{2}$ layer.[26–28] Rb, which is even weaker than H_2, is expected to have a very low critical coverage at low temperature. In contrast to this expectation, our data seem to indicate that more than two layers of ^{4}He can remain in the normal state on Rb even at $T=0$.

The maximum frequency shift $\Delta f_{\max}$ associated with the prewetting steps shown in Fig. 3 is a convenient measure of the normal coverage at superfluid onset. Figure 9 shows a plot of $\Delta f_{\max}$ for both forward and reverse isotherms as a function of temperature for surfaces 1 and 3. The solid straight line shows the expected value of δf from the KT theory, Eq. (2), which is equal to $\Delta f_{\max}$ if there is no dead layer. Like all of the other features of the isotherms, $\Delta f_{\max}$ is hysteretic. On the reverse isotherms, $\Delta f_{\max}$ seems to approach the KT line at the lowest accessible temperatures. On the forward isotherms, $\Delta f_{\max}$ has almost the same temperature dependence as the KT prediction, but it extrapolates to a remarkably high value of 2.0 layers at $T=0$. This can be compared to the typical onset behavior on gold, illustrated in Fig. 10, which shows two steps corresponding to the formation of 2 (presumably solid) layers followed by superfluid onset at essentially the same value of $\Delta f_{\max}$ we observe on Rb.

Discussion thus far has focused on the thin-to-thick transitions, but there also appears to be a qualitative change in behavior of the thin-film phase that occurs near 0.3 K and may conceivably be related to the transition reported by Wyatt, Klier, and Stefanyi.[13] Figure 11 shows the frequency shift for two isotherms at 0.2 and 0.4 K for surface 2. Both isotherms show a prewetting step and superfluid onset, but the thin phase ($\Delta\mu<-0.017$ K) is quite different in the two cases. The 0.2 K isotherm shows no shift in the frequency from the vacuum value until the prewetting step, while the 0.4-K isotherm has a continuously increasing value of Δf and a frequency shift of 0.2 Hz (corresponding to 0.8 layer) at the beginning of the prewetting transition. One possible explanation of this behavior is a superfluid[13] or other type of

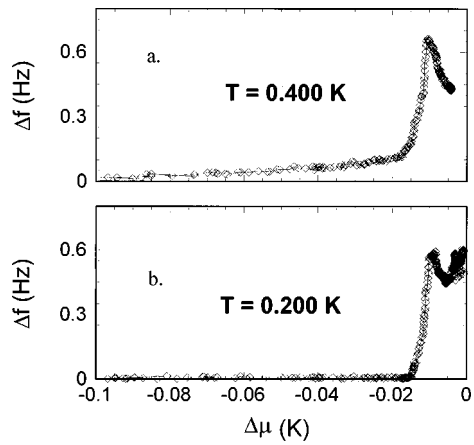

FIG. 11. Two isotherms showing the frequency shift as a function of chemical potential on Rb surface 2. There is a distinct difference in the thin-film states when comparing the isotherms above and below 0.3 K. The warmer isotherm (a) shows that there is a thin film whose thickness increases monotonically with $\Delta\mu$ that couples to the microbalance. In contrast, the colder isotherm (b) has no measurable film coupling to the microbalance until the prewetting transition at $-\Delta\mu=0.015$ K.

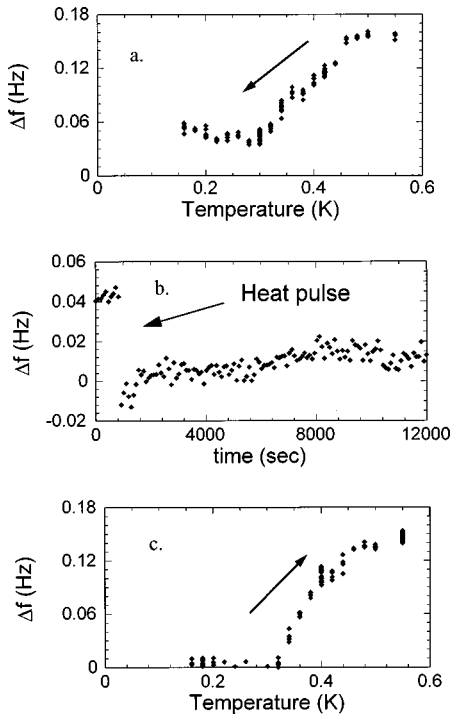

FIG. 12. Frequency shift of rubidium substrate 2 with a fixed amount of helium in experiment cell. (a) Frequency shift as a function of temperature as an isochore ranging from 0.55 to 0.16 K is performed. Between 0.5 and 0.3 K the frequency shift decreases, indicating an uncoupling of mass to the Rb surface. (b) Frequency shift as a function of time while the experiment is at 0.16 K. A heat pulse is applied to the microbalance to dry off the Rb surface. Immediately after the heat pulse the frequency shift returns to the vacuum state value. (c) An isochore with T increasing from 0.16 to 0.55 K. The frequency shift returns to the original value from *a*. In both isochores there is a distinct break in the slope at 0.3 K.

phase transition in the thin phase. Another possibility is that the observed differences are due to the fact that the saturated vapor pressure varies by more than a factor of 10^7 between 0.2 and 0.4 K, resulting in significantly different equilibrium times. To test the possible role of mass transfer kinetics, we measured isochores with both increasing and decreasing temperatures. We began with a vacuum at 0.55 K and added just enough helium to the cell to increase the chemical potential to a value below the prewetting transition so the adsorbed film would still be in a thin phase. The experiment was then cooled down to 0.2 K with this fixed amount of helium in the experiment [Fig. 12(a)]. As the experiment cooled, the frequency shift decreased indicating that the coupled mass to the microbalance was changing. This could either be due to helium leaving the microbalance or a transition to a thin superfluid film; it cannot be attributed to a mass-transfer bottleneck, since the normal film was present at high temperature. The film could be removed from the oscillator by applying a heat pulse to the microbalance at 0.2 K, as shown in Fig. 12(b). The frequency shift remained close to zero for several hours after the heat pulse. The temperature of the experiment was subsequently increased to 0.55 K and the microbalance frequency returned to its initial value as shown in Fig. 12(c). In both the heating and cooling cycles, 0.3 K marks a change in slope of Δf.

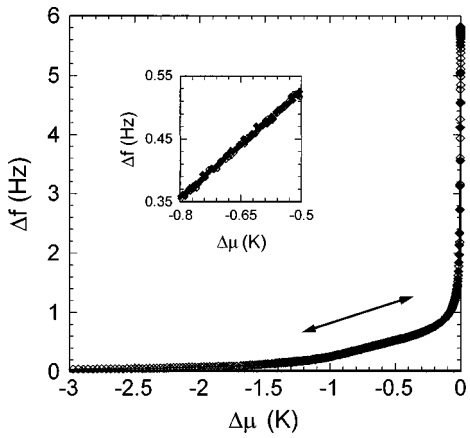

FIG. 13. Frequency shift for ^{3}He adsorption isotherms at 1.2 K on rubidium surface 2 as a function of chemical potential offset. Open diamonds correspond to the forward isotherm and solid diamonds to the reverse isotherm. The inset is a close-up of the data showing no hysteresis in the ^{3}He data in contrast to the ^{4}He data on exactly the same surface.

IV. DISCUSSION

The most striking feature of the phase diagram in Fig. 4 is the hysteresis in the prewetting thick/thin transition. Prewetting steps on Cs prepared in a similar way as the Rb surfaces described here are essentially identical in the forward and reverse directions.[8] On rough or porous surfaces, however, capillary condensation can give rise to hysteretic behavior on Cs.[29] We have ruled out this possibility on our substrates by carefully measuring isotherms using ^{3}He (for which neither wetting nor superfluidity is an issue) on substrate 2; there was no observable hysteresis and no excessive adsorption at saturation (Fig. 13), suggesting that the hysteresis we observe with ^{4}He is an intrinsic property of the ^{4}He surface phases, and not an artifact due to the substrate. Qualitatively similar hysteresis was observed on our surface 1. Demolder *et al.*[11] used a heat-flow technique to map the superfluid onset of ^{4}He on Rb at temperatures between 1.0 and 1.7 K. They also found that its position in the μ-T plane was hysteretic. Our measurements of the $\Delta\mu$ at onset for forward isotherms agree with their forward isotherms in the region where our data overlap. The width of the hysteresis in $\Delta\mu$ that they observe is considerably narrower than ours, possibly because their helium films are carrying a finite heat current.

Another significant difference between Rb and Cs is the width of the prewetting steps that are approximately three times wider on Rb than Cs. Below the prewetting critical temperature T_c^{pw}, prewetting is a first-order transition that ideally occurs at constant chemical potential, but even for $T > T_c^{\mathrm{pw}}$, maxima in the compressibility of the supercritical film give rise to broader steplike structures in isotherms. Monitoring the temperature dependence of the width of the transition is a standard method of locating the prewetting critical point.[8] In contrast to the Cs case, the width of the prewetting transitions on Rb is a smooth, almost linear function of temperature, with no obvious break in slope. These observations suggest that our Rb surfaces are more disordered than our Cs surfaces. The source of the substrate inhomogeneity is presumably variations in the wetting properties

of substrate patches with different crystallographic orientation.[30] If this is the case, then the observed hysteresis is associated with prewetting broadened by the effects of substrate inhomogeneity. In this interpretation, the reverse branch is due to a spinodal line (stability limit) of the thick-film superfluid phase. Our belief that the forward branch represents the equilibrium transition while the reverse branch is metastable is based on the fact that the Rb substrate is surrounded by strong binding surfaces (quartz and gold) that are covered with a thick superfluid film whenever the helium film on the Rb undergoes a thick/thin transition on either the forward or reverse isotherm. The thin-to-thick transition on the forward isotherm is nucleated at the edge of the Rb, while the thick-to-thin transition on the reverse isotherm requires a fluctuation and can therefore be supercooled. The reduction of hysteresis in the region near 1.95 K marks the remnant of the broadened prewetting critical point. Above 1.95 K, there is some remaining hysteresis in the prewetting transitions, but not in the position of the KT line. Prewetting is in the two-dimensional Ising universality class, and the phase transitions in this type of system are well known to be strongly affected by disorder,[31–34] while the KT transition, which is in the XY universality class, is relatively insensitive to disorder.[35]

The junction in the μ-T plane of the first-order prewetting line and the higher-order KT line shown in Fig. 4 has an unusual topology. Model calculations[36,37] show that the junction between a first-order and higher-order transition at a tricritical point usually occurs with no change in slope. Although the connection between the reverse transition (spinodal) and the KT line does appear to be smooth, the KT line meets the forward transition in a sharp, cusplike angle. Cusplike junctions in which the two transition lines meet tangentially are also allowed.[38,39]

Previous investigators have reached differing conclusions on the behavior of the superfluid onset transition at low temperatures. Demolder *et al.*[11] analyzed their results using an extrapolation scheme that properly accounted for the temperature dependences of the leading thermodynamic terms and concluded that the superfluid onset line does not intersect bulk liquid-vapor coexistence at a finite temperature. Wyatt, Klier, and Stefanyi[13] studied mass transport across a Rb surface for $0.1<T<0.35$ K in a region very close to coexistence ($\Delta\mu<0.006$ K). They interpret a jump in the critical superflow velocity to indicate a wetting temperature just above 0.3 K where a prewetting line joins the bulk liquid-vapor coexistence line. In terms of the surface energy balance, the difference between a 0.3-K wetting temperature and $T=0$ K prewetting is minuscule and might easily be due to very small differences in the surface chemistry.[40] Wyatt, Klier, and Stefanyi also suggest that both the thin and thick films along the prewetting lines are superfluid. In contrast, all of the Rb surfaces we investigated were wet at coexistence. Furthermore, the dissipation peak that is the hallmark of the KT transition was observed only in the thick phase. The behavior in the thin phase undergoes a subtle continuous change near $T=0.3$ K, which does not resemble the standard signature of either a superfluid onset transition or a first-order transition with a discontinuity in the film thickness.

It is useful to compare the superfluid transition observed on Rb with superfluid onset on conventional substrates and Cs, as shown in the schematic d-T phase diagrams shown in Fig. 14. Figure 14(a) shows the phase diagram for ^{4}He adsorbed on a conventional substrate such as Mylar or gold. The helium film exists in only two states, superfluid (S) and normal (N), which are separated by the dashed KT line. The $d>0$ intercept at $T=0$ corresponds to the dead layer. The linear dependence of d on T at low temperature is very similar to that given by Eq. (2), while the divergence at T_λ is due to finite-size effects, with $d\sim t^{-0.67}$. Figure 14(b) shows the combined prewetting/superfluid onset phase diagram for ^{4}He on Cs. Cs substrates thicker than approximately 3 layers have a wetting temperature $T_W>0$. For $0<T<T_W$, a thin phase can coexist with bulk liquid. For $T_W<T<T_c^{pw}$, there is a range of film thickness that is unstable. The KT line is almost exactly the same as in Fig. 14(a), except that it terminates at a critical end point when it collides with the range of unallowed d. For temperatures below the critical end point, the signatures of the KT transitions are not observed[9] because the film never attains the critical onset thickness. A candidate phase diagram that summarizes our observations of superfluid onset on Rb is shown in Fig. 14(c), which

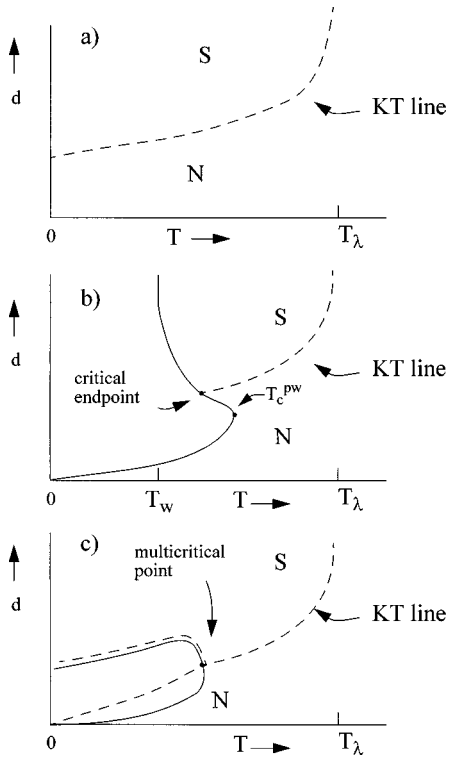

FIG. 14. Schematic phase diagrams in the film thickness d vs T plane. (a) A typical strong-binding substrate showing the dashed KT line. The thickness at $T=0$ is due to a dead layer of helium. The slope is linear at low T and diverges near T_λ. (b) Phase diagram for cesium showing the coexistence of two films of different thicknesses between the wetting temperature T_w and the prewetting critical point T_c^{pw}. For temperatures below T_w only a thin film exists. On cesium substrates, the KT line terminates at a critical end point. (c) A possible phase diagram that models our rubidium data. Notice that there is no wetting temperature and below a multicritical point there is a region of unstable thickness enclosed by the solid line. The KT line passes through the multicritical point and splits into two branches, one of which follows the upper phase boundary while the other goes through the region of unstable thickness.

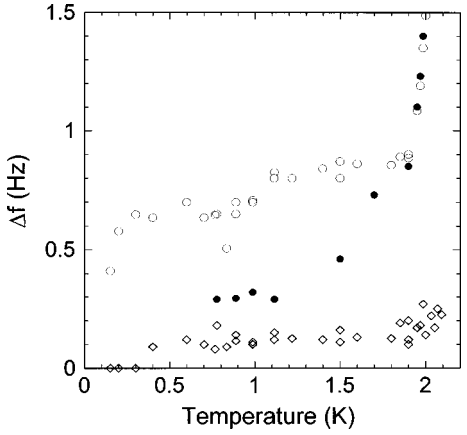

FIG. 15. Phase diagram in the thickness-temperature plane for ^{4}He films on Rb substrate number 2. Open circles are $\Delta f_{\max}$ for the forward isotherms and the solid ones are the corresponding $\Delta f_{\max}$ for the reverse isotherms. Diamonds indicate the thickness of the thin film at the prewetting transition. Note the abrupt change in the thin-film thickness near 0.3 K.

should be compared to the data in Fig. 15. In this case, there is no wetting temperature, but there is a prewetting transition, which corresponds to a range of unstable thickness. The hysteresis we observe is due to metastable states between the phase boundary and the spinodal line. On the forward isotherms, the transition takes place at the upper phase boundary, while on the reverse isotherms, the transition takes place on the lower spinodal line. Where the spinodal line and the phase boundary meet marks the end of hysteresis at a critical point. In this case, however, the KT line intersects the prewetting phase boundary very close to the prewetting critical point. Since both the thickness and the superfluid order parameter are singular there, it is presumably a multicritical point. The resulting phase diagram resembles the well-known bulk ^{3}He-^{4}He mixture phase diagram (with d playing the role of ^{4}He concentration) that also has a multicritical point where the lambda line hits the phase separation curve.

The fact that the standard signatures of a KT transition (superfluid jump and dissipation peak) are observed all along the prewetting line implies that the KT line does not stop at the multicritical point, but rather continues along the upper phase boundary and along the spinodal. This is surprising because the physics that determines the prewetting behavior and the superfluid transition is ordinarily quite distinct, and it is not obvious why the two transitions should not be completely independent. Apparently, on Rb the combination of the multicritical point and the substrate disorder merge the two phenomena into a single strongly coupled transition.

Although the positions of the features that mark the surface phase transitions are quite reproducible from one Rb sample to another, the size and shape of the features vary considerably, and as noted above, cannot be simply explained by the standard KT model. The discrepancies in the superfluid jump are particularly puzzling since the predicted value, which is universal, has been experimentally verified on a number of substrates. It should be noted that in any oscillator experiment, particularly at low temperature, a potential source of error in measurements of δf is the superfluid coupling factor k of Eq. (1). In systems in which k approaches 1, such as exfoliated graphite studied in Ref. 21, the observed values of δf are very small because the oscillator couples to almost all of the fluid even when it is superfluid. The data can be corrected for this effect by multiplying the observed values of δf by $1/(1-k)$. The values of the superfluid jumps corrected using this procedure agree with the KT prediction even for exfoliated graphite, where the correction can be as large as a factor of 50.[21] We have not applied such a correction to our Rb data (equivalent to choosing $k=0$ on Rb), so the values of δf shown in Figs. 3 and 7 are lower bounds. It is interesting to note that even this lower bound for δf is often considerably larger than the KT prediction.

The KT predictions for the dissipation are not universal, although the dissipation is expected to be proportional to the temperature.[3] This trend has been observed in systems with thick helium films at relatively high temperature,[4,18] but experiments at lower temperature[25,21] show anomalies in both the height and the width of the peaks that cannot be explained by the standard theory.[3] Dissipation measurements using an oscillating substrate are subject to the same corrections for the superfluid coupling factor as discussed above, so our values of ΔR again represent a lower bound.

V. CONCLUSIONS

Although the substrate potential in Rb is only 5% stronger[10] than Cs, the behavior of helium films on the two substrates is surprisingly different. The difference is presumably due to differences in the topology of the underlying phase diagram and in the degree of substrate disorder. In Cs, the KT line terminates on a noncritical point, while in Rb, the KT line seems to meet the prewetting line near a critical region. Hysteretic prewetting on Rb was observed in all of our samples as well as by other investigators[11,14] and seems to be a robust feature of prewetting on Rb. Perhaps the most important result of the experiments reported here is that the hysteresis ends at the critical point. This, together with the fact that the thick/thin transition always seems to occur between films in the normal state implies that superfluidity and prewetting are strongly coupled on Rb. This interaction yields an unusual superfluid transition that is not of the Kosterlitz-Thouless type. This type of behavior may be typical of a range of ''intermediate'' strength substrates characterized by prewetting (or layering) transitions without accompanying wetting transitions.

Another surprising feature of superfluid onset on Rb substrates is that helium films with an average coverage of more than two layers can remain normal on Rb even at very low temperatures. The normal film is not inert, however. Once superfluidity is established, less than one layer is viscously locked to the substrate. We have also observed unusual phenomena in the thin phase near 0.3 K, but our results cannot be simply explained in terms of a superfluid/normal transition in the thin phase. The interpretation of our primary data depends somewhat on assumptions about the coupling of the superfluid fraction of the film. The fact that the super/normal and thick/thin transition are so tightly intertwined and that the bottom layers are not inert makes it difficult to determine the total film coverage near the transition, since our oscillators couple to a combination of the normal and superfluid

part of the film that in principle depends on the coverage. To remove this ambiguity we are developing oscillators that have displacements normal to the surface and therefore directly determine the total coverage.

ACKNOWLEDGMENT

This work was supported by NSF Grant No. DMR 9623976.

[1] D. F. Brewer, in *The Physics of Liquid and Solid Helium*, edited by K. H. Bennemann and J. B. Ketterson (Wiley, New York, 1978), Pt. II; J. D. Reppy, in *Phase Transitions in Surface Films*, edited by J. G. Dash and J. Ruvalds (Plenum, New York, 1980).
[2] M. Kosterlitz and D. Thouless, J. Phys. C **6**, 1181 (1973).
[3] V. Ambegaokar, B. I. Halperin, D. R. Nelson, and E. D. Siggia, Phys. Rev. B **21**, 1806 (1980).
[4] D. J. Bishop and J. D. Reppy, Phys. Rev. B **22**, 5171 (1980).
[5] G. Agnolet, S. L. Teitel, and J. D. Reppy, Phys. Rev. Lett. **47**, 1537 (1981).
[6] J. Maps and R. B. Hallock, Phys. Rev. Lett. **47**, 1533 (1981).
[7] E. Cheng, M. W. Cole, W. F. Saam, and J. Treiner, Phys. Rev. B **46**, 13 967 (1992).
[8] J. E. Rutledge and P. Taborek, Phys. Rev. Lett. **69**, 937 (1992).
[9] P. Taborek and J. E. Rutledge, Phys. Rev. Lett. **71**, 263 (1993).
[10] A. Chizmeshya, M. W. Cole, and E. Zaremba, J. Low Temp. Phys. **110**, 677 (1998).
[11] B. Demolder, N. Bigelow, P. J. Nacher, and J. Dupont-Roc, J. Low Temp. Phys. **98**, 91 (1995).
[12] G. Mistura, H. C. Lee, and M. H. W. Chan, Physica C **194**, 661 (1994).
[13] A. F. G. Wyatt, J. Klier, and P. Stefanyi, Phys. Rev. Lett. **74**, 1151 (1995).
[14] T. A. Moreau and R. B. Hallock, J. Low Temp. Phys. **110**, 659 (1998).
[15] M. Schick and O. E. Vilches, Phys. Rev. B **48**, 9910 (1993).
[16] M. Chester and L. C. Yang, Phys. Rev. Lett. **23**, 1377 (1973).
[17] D. S. Spencer, M. J. Lea, and P. Fozooni, Phys. Lett. **109A**, 295 (1985).
[18] R. Brada, H. Chayet, and W. I. Glaberson, Phys. Rev. B **48**, 12 874 (1993).
[19] D. Ross, J. E. Rutledge, and P. Taborek, Phys. Rev. Lett. **76**, 2350 (1996).
[20] D. Ross, P. Taborek, and J. E. Rutledge, Phys. Rev. Lett. **74**, 4483 (1995).
[21] P. A. Crowell and J. D. Reppy, Phys. Rev. B **53**, 2701 (1996).
[22] K. S. Ketola and R. B. Hallock, Phys. Rev. Lett. **71**, 3295 (1993).
[23] D. Salt, *Handbook of Quartz Crystal Devices* (Van Nostrand Reinholdt, New York, 1987).
[24] D. Ross, J. A. Phillips, J. E. Rutledge, and P. Taborek, J. Low Temp. Phys. **106**, 81 (1997).
[25] G. Agnolet, D. F. McQueeney, and J. D. Reppy, Phys. Rev. B **39**, 8934 (1989).
[26] P. J. Shirron and J. M. Mochel, Phys. Rev. Lett. **67**, 1118 (1991).
[27] P. W. Adams and V. Pant, Phys. Rev. Lett. **68**, 2350 (1992).
[28] D. Tulimieri, N. Mulders, and M. H. W. Chan, J. Low Temp. Phys. **110**, 609 (1998).
[29] K. S. Ketola, S. Wang, and R. B. Hallock, Phys. Rev. Lett. **68**, 201 (1992).
[30] M. W. Cole, M. R. Swift, and F. Toigo, Phys. Rev. Lett. **69**, 2682 (1992).
[31] G. Forgacs, R. Lipowsky, and T. M. Niewenhuizen, in *Phase Transitions and Critical Phenomena*, edited by C. Domb and J. Lebowitz (Academic, New York, 1991), Vol. 14, p. 136.
[32] A. Falicov and A. N. Berker, Phys. Rev. Lett. **76**, 4380 (1996).
[33] R. Blossey, T. K. Kinoshita, and J. Dupont-Roc (unpublished).
[34] R. Blossey, T. K. Kinoshita, X. Muller, and J. Dupont-Roc, J. Low Temp. Phys. **110**, 665 (1998).
[35] J. V. Jose, Phys. Rev. Lett. **46**, 1591 (1981).
[36] R. Pandit, M. Schick, and M. Wortis, Phys. Rev. B **26**, 5112 (1982).
[37] S. Ostlund and A. N. Berker, Phys. Rev. B **21**, 5410 (1980).
[38] I. D. Lawrie and S. Sarbach, in *Phase Transitions and Critical Phenomena*, edited by C. Domb and J. L. Lebowitz (Academic, New York, 1984), Vol. 9, p. 1.
[39] M. Schick (private communication).
[40] B. Demolder and J. Dupont-Roc, J. Low Temp. Phys. **104**, 359 (1996).